

Comparison of whole liver and small region-of-interest measurements of MRI liver R2* in children with iron overload

M. Beth McCarville · Claudia M. Hillenbrand ·
Ralf B. Loeffler · Matthew P. Smeltzer · Ruitan Song ·
Chin-Shang Li · Jane S. Hankins

Received: 23 October 2009 / Revised: 14 January 2010 / Accepted: 29 January 2010 / Published online: 24 March 2010
© Springer-Verlag 2010

Abstract

Background Measurement of liver MRI T2* and R2* is emerging as a reliable alternative to liver biopsy for the quantitation of liver iron content. A systematic investigation of the influence of the region-of-interest size and placement has not been conducted.

Objective To compare small and whole liver region-of-interest (ROI) MRI R2* values to each other and to biopsy liver iron content in patients with iron overload.

Materials and methods Forty-one iron-overloaded patients, ages 7–35 years, underwent biopsy for liver iron content quantitation and MRI for liver R2* measurement within 30 days. Three reviewers independently used small and whole liver ROIs to measure R2*. Inter-reviewer agreement

was assessed with the intra-class correlation coefficient (ICC). Associations between R2* and liver iron content were investigated using Spearman's rank-order correlation and Monte Carlo estimated exact *P* values.

Results Biopsy liver iron content and small and whole liver ROI R2* measurements were strongly associated for all reviewers (all $P < 0.0001$). Although inter-reviewer agreement was excellent for both ROI methods (ICC=0.98–0.99), the small ROI technique more frequently led to inter-reviewer differences larger than 75 Hz, slightly higher R2* values, larger standard errors and greater range in values.

Conclusion Small and whole liver ROI techniques are strongly associated with biopsy liver iron content. We found slightly greater inter-reviewer variability in R2* values using the small ROI technique. Because such variability could adversely impact patient management when R2* values are near a threshold of iron chelation therapy, we recommend using a whole liver ROI.

M. B. McCarville (✉) · C. M. Hillenbrand · R. B. Loeffler ·
R. Song

Department of Radiological Sciences,
St. Jude Children's Research Hospital,
262 Danny Thomas Place, Mail Stop 210,
Memphis, TN 38105, USA
e-mail: beth.mccarville@stjude.org

M. B. McCarville
Department of Radiology,
The University of Tennessee College of Medicine,
Memphis, TN, USA

M. P. Smeltzer · C.-S. Li
Department of Biostatistics,
St. Jude Children's Research Hospital,
Memphis, TN, USA

J. S. Hankins
Department of Hematology,
St. Jude Children's Research Hospital,
Memphis, TN, USA

Keywords MRI · Sickle cell anemia · Iron overload ·
Liver iron content

Introduction

Chronic red blood cell transfusion therapy has greatly improved survival and quality of life of patients with inherited and secondary refractory anemias, ineffective erythropoiesis, and those with severe hemolysis [1, 2]. However, the associated iron load damages vital structures including the heart, liver and endocrine organs, the severity of which increases with increased duration of transfusion therapy (i.e. the iron burden). Iron chelation therapy can diminish organ damage but has its own toxicities and complications if not

monitored carefully. Because iron is essential for many physiologic functions, the goal of therapy is to reduce toxicity from excessive iron while minimizing toxicity associated with iron chelation [1]. Noninvasive quantitative assessment of liver and myocardial iron by means of MRI liver-to-muscle signal intensity ratios and R2 and R2* relaxometry ($R2=1/T2$, $R2^*=1/T2^*$) have emerged as reliable alternatives to liver biopsy to monitor body iron content because good correlations with biopsy-proven liver iron content have been observed [3–17].

Since the first clinical investigations of MRI signal intensity and decay measurements for estimation of liver iron content, most investigators have used small (0.5–3 cm) regions of interest (ROIs) placed in an area of the liver appearing homogeneous and devoid of vessels [4, 10, 12, 14–16, 18–24]. While measurements obtained with this approach have shown excellent correlations with biopsy specimen liver iron content, the method is subject to several potential pitfalls [3, 10, 12, 14–17]. Placement of the ROI is subjective leading to inter-reviewer variability. Furthermore, the distribution of liver iron, in patients with iron overload, is likely not uniform, making both liver biopsy and small ROI measurements prone to sampling error [8, 25–28]. Several investigators have reported the use of a whole liver ROI method to measure liver R2 and R2*, which may provide a more accurate assessment of overall liver iron content [9, 29, 30]. A systematic investigation of the influence of the ROI size and placement, however, has not been conducted. The purpose of our study was to compare small and whole liver ROI R2* measurements with each other and with biopsy-proven liver iron content in patients with iron overload in an effort to determine the best method for noninvasive liver iron quantitation using MRI.

Materials and methods

Patient selection

This prospective study was approved by our Institutional Review Board and was performed with HIPPA compliance. Because patients had to follow breath-holding instructions for MRI, only those ≥ 7 years of age and not requiring sedation or general anesthesia for MRI were eligible. A diagnosis of iron overload, defined as serum ferritin $\geq 1,000$ ng/L within 3 months before study enrollment or a history of ≥ 18 red blood cell (RBC) transfusions, and a clinical need for liver biopsy to monitor iron overload were required [31, 32]. In accordance with our institutional MRI safety policy, pregnant females and patients with internal ferromagnetic material were not eligible. Eligible patients or their legal guardian signed consent and assent as appropriate. The association

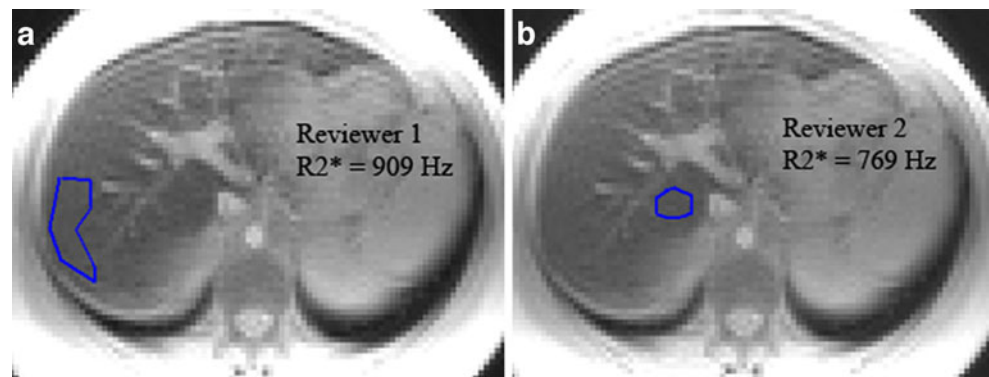
between small ROI R2* measurements and liver iron content, from this study, have been previously published [3].

MRI scanning and region-of-interest procedures

To avoid potential variability in R2* measurements resulting from differences in MRI equipment, all patients were scanned on the same 1.5-T Siemens Symphony (Malvern, PA) MRI scanner. With a phased-array body coil, a single breath-hold technique was used to obtain 20 non-contrast-enhanced gradient echo axial images at the level of the main portal vein with a repetition time (TR) of 200 ms and 20 increasing echo times (TE). Echo times ranged from 1.1 ms–17.3 ms at 0.08 ms increments. Other imaging parameters were 25-degree flip angle, 10-mm slice thickness, 3.125 mm in plane resolution and 1,950 Hz bandwidth, $128 \times (96\text{--}128)$ matrix and $380 \text{ mm} \times (285 \text{ mm--}380 \text{ mm})$ field of view. Total acquisition time for the 20 images ranged from 18 to 25 s.

Images were transferred to a computer workstation for post-processing. Quantitative T2* maps of the entire cross-sectional area of the liver (at the level of the main portal vein) were calculated using custom-written MATLAB (MathWorks, Natick, MA) software and the signal intensity drop over the image series was fitted on a pixel-by-pixel basis to a monoexponential decay using the least-squares fit method [33]. Region-of-interest T2* measurements were then obtained independently by three reviewers—one radiologist with 14 years of experience in pediatric radiology (MBM) and two MRI physicists with 14 years (CMH) and 4 years (RS) of experience in MRI. The reviewers were blinded to patient history, liver iron content and the other reviewers' T2* measurements. Each reviewer performed ROI analyses in two ways: (1) A small ROI, of at least 1-cm diameter, was manually drawn in an area of the liver that appeared homogeneous and was devoid of vessels on the T2*W images or the calculated T2* map (Fig. 1). To simulate current standard of practice reviewers determined the shape, size and location of ROIs at their own discretion, based on personal experience. Because liver biopsies were obtained from the right lobe of the liver, ROIs were placed in the right lobe when possible. (2) To avoid potential bias resulting from knowledge of small ROI T2* values, each reviewer waited 3 months before performing whole liver ROI analyses. The whole liver analyses were performed by manually drawing an ROI just inside the outer margins of the liver, outlining the entire cross-sectional area, including vessels (Fig. 2). A T2* histogram was obtained from the ROI and outliers in the histogram (values corresponding to vessels rather than liver parenchyma) were removed by rejecting T2* values above those from within the area under the main peak (Fig. 2). An image overlay of pixels included in the adjusted T2* calculation was used to confirm that major vessels were excluded (Fig. 2). To ensure that an

Fig. 1 Hb SS sickle cell anemia in a 6-year-old boy. Axial gradient echo MRI (TR 200 ms, TE 1.1 ms) shows small ROIs drawn by two reviewers in different areas of the liver that resulted in substantially different $R2^*$ values



adequate number of pixels were analyzed within the ROI, we excluded children whose number of fitted pixels (i.e., those included in the $T2^*$ determination) was <25% of all pixels within the ROI by any one reviewer using either ROI technique. A fitted pixel count <25% can occur when the ROI contains a large amount of tissue that has $T2^*$ signal decay that is too rapid to be quantitated (such as heavily iron-laden liver). For both ROI techniques the mean $T2^*$ within the ROI was converted into the corresponding $R2^*$ [Hz] using the formula $R2^* = 1,000/T2^*[\text{ms}]$. We used the $R2^*$ value because it is directly proportional to the liver iron content (higher liver iron content = higher $R2^*$) which eases interpretation of results and is more intuitive than $T2^*$ (higher liver iron content = lower $T2^*$).

Liver biopsy

All children underwent percutaneous liver biopsy within 30 days after MRI. Biopsies were performed after MRI to avoid the potential impact of metal fragments from the biopsy needle on $R2^*$ measurement. Biopsies were performed by an interventional radiologist using a co-axial percutaneous, transcapsular or transjugular technique and a 17-gauge sheath. Three passes were made to obtain tissue for histologic review, liver tissue iron quantitation and RNA microarray analysis. To reduce post-procedural bleeding, the latter technique was performed on children with increased risk of bleeding, such as thrombocytopenia or prolonged bleeding time [34]. Biopsy specimens measuring at least 5 mm in length were obtained, placed in a metal-free vial, refrigerated and sent to Mayo Clinic Laboratory (Rochester, MN) for liver iron quantitation. Liver iron content in biopsy tissue was considered the reference standard for liver iron quantitation and was compared to small and whole liver ROI $R2^*$ values.

Quantitation of liver iron content

Liver tissue iron quantitation was performed using acid digestion followed by inductively coupled plasma-mass spectrometry (ICP-MS) analysis as previously described [35].

Statistical analysis

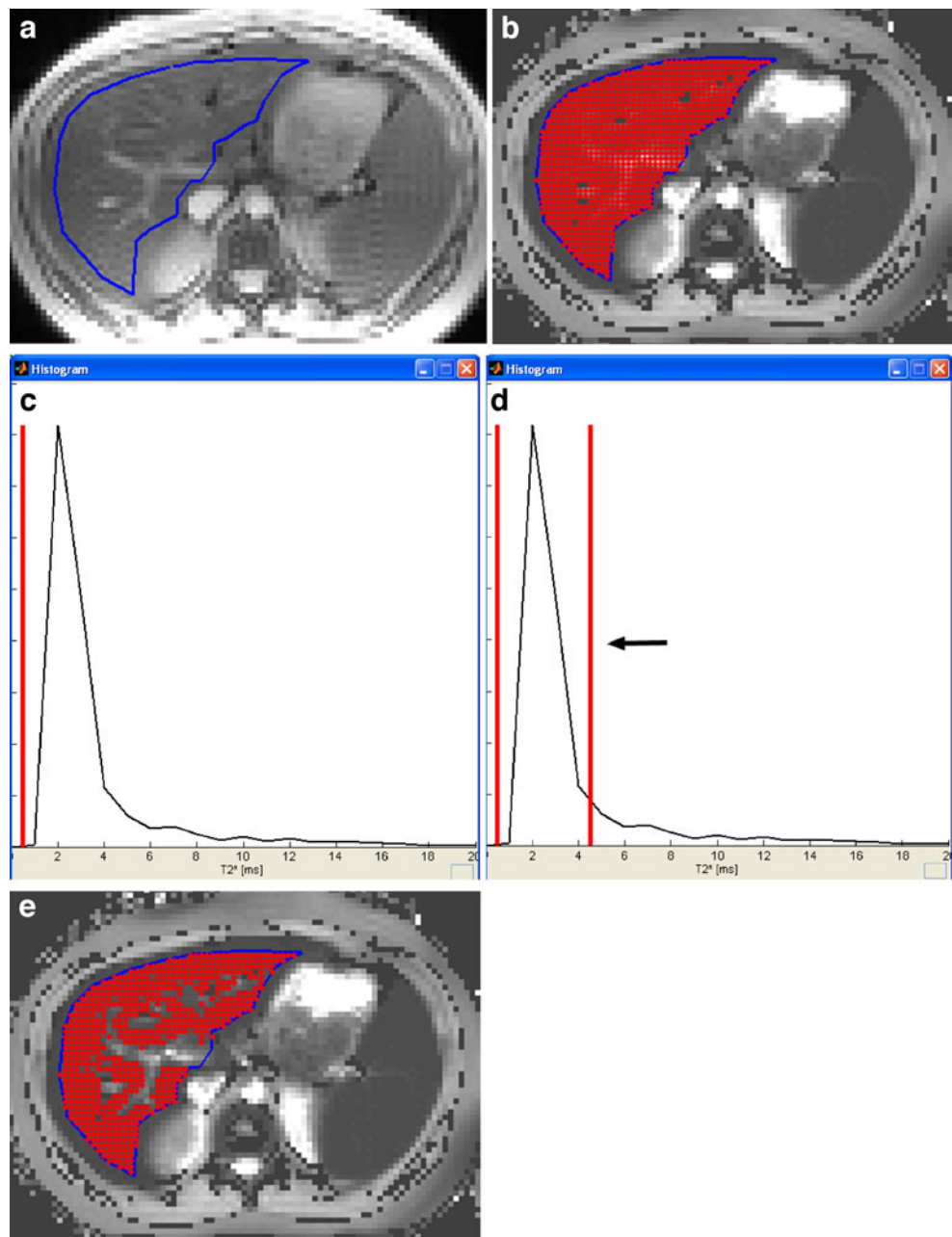
After $T2^*$ from small and whole liver ROIs were transformed into reciprocal $R2^*$ values, the intra-class correlation coefficient (ICC) was used to assess the agreement among $R2^*$ measurements by the three reviewers. Relationships between $R2^*$ values and liver iron content and percentage fitted pixels were investigated using Spearman's rank-order correlation; Monte Carlo estimated exact P values are reported. P values ≤ 0.05 were considered significant. Robust linear regression modeling was used to fit the line and 95% confidence interval for predicting liver iron content with $R2^*$ for small and whole liver ROIs.

Results

Demographics, clinical characteristics and laboratory findings

Fifty-two children were enrolled from October 2005 through June 2007. Two children with underlying medical conditions precluding non-sedated MRI and one with internal metal were withdrawn from the study before any protocol-driven tests were performed. Of the remaining 49, 8 were excluded from data analysis, 5 because there were <25% fitted pixels within the ROI (3 on both small and whole liver ROI analyses, 2 on whole liver ROI only), 1 had an inadequate biopsy, 1 was unable to breath-hold and 1 was claustrophobic (no imaging was obtained on this patient). All participants tolerated liver biopsy without complication: 35 underwent percutaneous, transcapsular biopsy and 6 had transjugular biopsy due to increased risk of bleeding. The 41 evaluable patients ranged in age from 7 to 35 years (mean, 15.5 years); 22 were male (54%). Primary diagnoses were sickle cell anemia (Hb SS) ($n=28$), β thalassemia major ($n=5$), Hb S/ β thalassemia ($n=2$), congenital hypoplastic anemia ($n=2$), and sideroblastic anemia, glioblastoma multiforme, paroxysmal nocturnal hemoglobinuria and Hb E thalassemia ($n=1$ each). These patients had each received an average of 94 RBC trans-

Fig. 2 Diamond Blackfan anemia in a 17-year-old boy. The whole liver ROI analyses were performed by first (a) drawing a ROI just inside the outer margins of the liver as shown in this axial MR gradient echo image (TR 200 ms, TE 1.1 ms). **b** This unadjusted pixel overlay on the T2* map shows that almost all pixels (in red) in the ROI are included in the T2* calculation as shown in (c). **c** The corresponding line histogram shows the distribution of signal intensities of all red pixels shown in (b). The y axis reflects the number of pixels per T2* species. In this example the calculated T2* would be the mean of all T2* values between the minimum value, 0.5 ms (red vertical line), and maximum value, 20 ms. **d** The reviewer adjusts the maximum measured T2* (arrow) by lowering it to include only the area under the major peak and exclude higher T2* values coming from vessels. **e** The adjusted pixel overlay is used to confirm that vessels were excluded from the mean T2* calculation



fusions (range 7–425 transfusions). Four patients had received <18 RBC transfusions but met study criteria because their serum ferritin was $\geq 1,000$ ng/mL within 3 months of study entry. By tissue biopsy, the liver iron contents ranged from 0.6–27.6 mg Fe/g liver dry weight (mean, 10.3 mg Fe/g; normal range = 0.2–2.4 mg Fe/g liver dry weight). Two children had normal liver iron contents. The five children excluded for <25% fitted pixels had liver iron contents ranging 19.7–38.8 mg Fe/g liver dry weight (mean 27.7 mg Fe/g liver dry weight). Two of these five had <25% fitted pixels on whole liver ROI analysis but >25% on small ROI. These two had the lowest liver iron contents in this subset: 24.6 and 19.7 mg Fe/g liver dry weight.

Small and whole liver ROI R2* results and comparison with the reference standard

Summary statistics for small and whole liver ROI R2* measurements for each reviewer are shown in Table 1. Compared to the whole liver ROI technique, the small ROI method resulted in slightly higher R2* values and larger standard errors for all three reviewers and a greater range between maximum and minimum values for two reviewers. There was a strong association between the reference standard, liver iron content, and small ROI and whole liver ROI R2* measurements for all three reviewers (Table 2). The scatter plots from robust linear regression analysis

Table 1 R2* values for 41 small and whole liver ROI analyses for three reviewers. All measurements are in Hz

	Reviewer	Mean R2* (Std. error)	R2* range (min, max)
Small ROI	1	383 (34)	832 (77, 909)
	2	387 (33)	755 (78, 833)
	3	373 (34)	833 (76, 909)
Large ROI	1	346 (29)	705 (64, 769)
	2	349 (30)	768 (66, 833)
	3	350 (30)	702 (67, 769)

(Fig. 3, reviewer 1 shown) clearly show that the association between liver iron content and R2* measurements was strongest at lower liver iron content and R2* values and progressively decreased at higher values (especially above 25 mg Fe/g) by both ROI techniques. The R2* values were inversely, significantly, associated with the number of fitted pixels (correlation coefficient = -0.64 , $SE=0.11$; $P<0.001$) such that higher R2* values resulted in fewer fitted pixels (Fig. 4). We noted an uneven distribution of fitted pixels on whole liver ROI pixel overlays with increasing R2* values (Fig. 4). Utilizing the small ROI technique resulted in differences in the size, configuration and placement of the ROI between reviewers that more frequently led to differences ≥ 75 Hz (Table 3; Fig. 1). Even so, inter-reviewer agreement was excellent for both small and whole liver ROI methods (Table 4). There was also a strong association between small and whole liver ROI R2* measurements for each reviewer (Table 5).

Discussion

We found a strong association between liver iron content and R2* values using both small and whole liver ROI analyses. The association, however, becomes weaker at higher values regardless of the ROI technique used. We also showed that as R2* values increase, the number of fitted pixels within a ROI decreases. Such pixel drop-out

occurs in areas of the liver containing very high iron concentration causing extremely rapid T2* signal decay that cannot be quantitated [21]. The relation between R2* and pixel drop-out likely explains the stronger association between R2* and liver iron content at lower values since relatively more pixels are included in the R2* calculation. As pixels are excluded from R2* calculation the distribution of fitted pixels in the liver can be uneven. In our study, this heterogeneity became obvious on the whole liver ROI T2* pixel overlay. Our findings agree with others who have assessed the distribution of R2* and R2 signal within livers of patients with iron overload [5, 8, 11]. In their study of 105 patients with a variety of liver diseases, St. Pierre and colleagues [8] found increasing R2 variability throughout the liver with increasing liver iron content. Others have shown directly, by histologic inspection of biopsy material obtained from various locations in livers resected from patients with end-stage liver disease, that the heterogeneity of iron deposition increases with increasing liver iron content [25–28]. Therefore, patients with iron overload (for whom MRI is increasingly used to monitor liver iron content noninvasively) are likely to have varying degrees of uneven liver iron distribution. Subsequently, relative to a whole liver ROI measurement, the small ROI method and liver biopsy are likely more prone to sampling variability, especially in children with high liver iron content.

Due to inter-reviewer variability in size, shape and placement of the small ROI, coupled with inherent liver signal inhomogeneities, it is perhaps not surprising that we found a broader range in small ROI R2* values relative to whole liver values for two reviewers. Importantly, the number of cases with R2* values differing by more than 75 Hz between reviewers was greater when using the small ROI technique. In clinical practice, such variability could adversely impact the management of iron-overloaded patients when R2* values are near the threshold to initiate iron chelation management (liver iron content above 5–7 mg Fe/g liver dry weight) or the threshold to implement more aggressive iron chelation due to increased risk of cardiac dysfunction (liver iron content consistently above 15 mg Fe/g liver dry weight) [31, 36]. In contrast to the small ROI method, placement of the whole liver ROI is less subjective, since the operator is guided by the outer borders

Table 2 Spearman's correlation between liver R2* measurements and the reference standard, tissue specimen liver iron content, using a small and whole liver ROI method for each of three reviewers

Reviewer	Correlation coefficient	Standard error	P value
Small ROI method			
1	0.97	0.01	<0.0001
2	0.96	0.02	<0.0001
3	0.96	0.02	<0.0001
Whole liver ROI method			
1	0.96	0.02	<0.0001
2	0.97	0.01	<0.0001
3	0.96	0.01	<0.0001

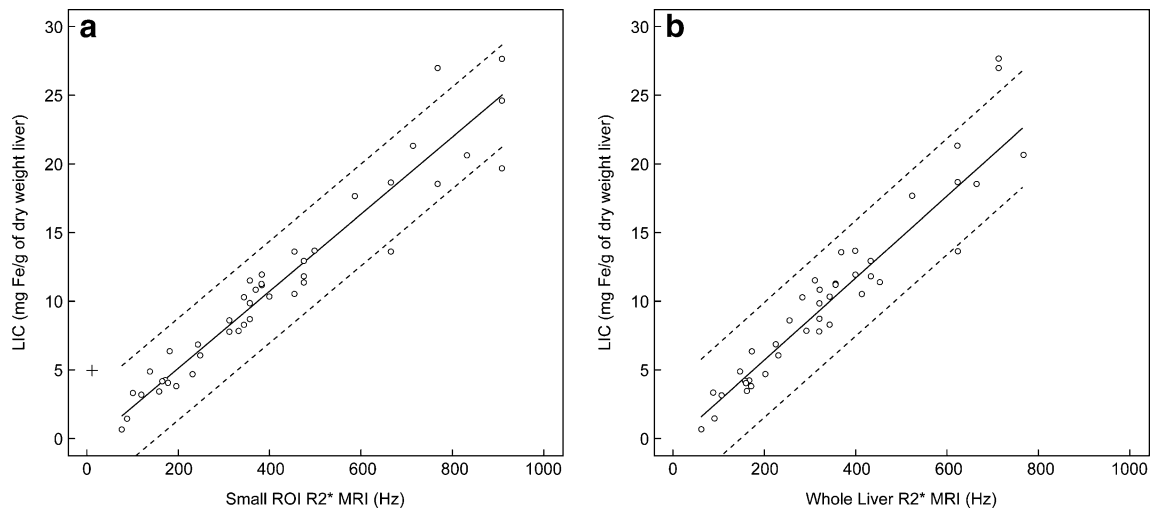


Fig. 3 Scatter plots show robust linear regression line (solid) and 95% prediction limits (dotted lines) of the association between biopsy-proven liver iron content and MRI R2* values using (a) a small ROI

and (b) whole liver ROI. Note strong association at lower values and weaker association at higher values by both techniques

of the liver. However, choice of the maximum T2* value to include in the whole liver ROI analysis is operator-dependent and can vary between reviewers. Despite this, we found smaller ranges and standard errors in whole liver ROI R2* values. Our findings are in agreement with those of Positano et al. [29], who found larger differences in T2* measurements using a small ROI method than with a whole liver automated ROI method. Those investigators used an elaborate model based on a fuzzy clustering algorithm and T2* imaging obtained from a phantom and 40 patients with

beta thalassemia to exclude vessels from automated whole liver T2* measurements. Our whole liver ROI method has the benefit of using the patient’s own imaging and is simpler to utilize.

Of the 49 children who underwent MRI for our study, about 13% (5/49) were excluded because there were <25% fitted pixels in either the small (n=3) or whole liver ROI (n=5, 3 of whom also had <25% fitted pixels using a small ROI). This occurred in children with very high liver iron content. This technical failure rate is similar to the 16% (7/

Fig. 4 These axial MRI T2* maps show decreases in fitted pixels (in red) with increasing R2* values a 83% fitted pixels; R2*=86 Hz. b 47% fitted pixels; R2*=699 Hz. c 24% fitted pixels; R2*=716 Hz. d 7% fitted pixels; R2*=837 Hz. Note uneven distribution of fitted pixels with increasing R2*

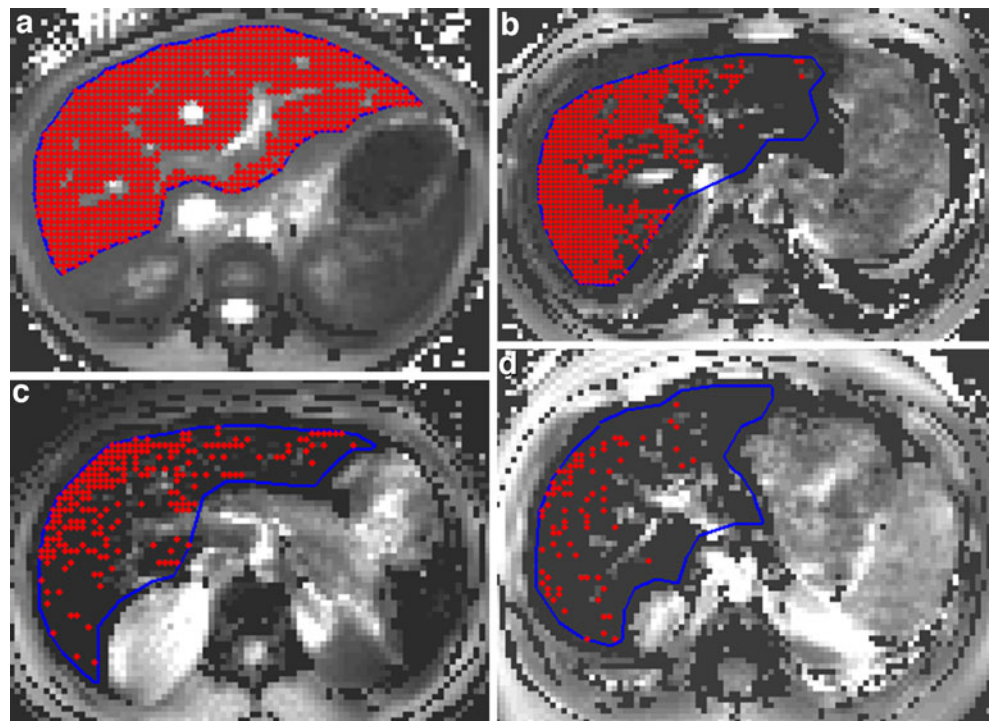


Table 3 The number of cases with increasing differences in R2* values among three reviewers by small and whole liver ROI analysis. Note that two cases were excluded from the whole liver ROI analysis due to <25% fitted pixels

Maximum differences in R2* values among three reviewers (Hz)	Number of cases on small ROI analysis	Number of cases on whole liver ROI analysis
0–25	31	29
26–50	5	7
51–75	1	2
76–100	2	1
>100	4	2
Total	43	41

44) reported by Virtanen et al. [21] due to poor signal-to-noise ratios caused by high liver iron content when comparing small liver ROIs to paraspinal muscle R2* measurements. We found that when a whole liver ROI analysis resulted in an inadequate number of fitted pixels, a small ROI analysis offered an alternative approach. In such cases, an area of liver containing an adequate number of fitted pixels can be identified using the whole liver pixel overlay and a small ROI can be placed within it. The result must be interpreted with caution, however, because the R2* value will be an underestimate since the ROI was intentionally placed in an area with less pixel drop-out, hence lower iron content than surrounding liver. In the future, we will investigate other pulse sequences, such as gradient-echo sampling of free induction decay and echo (GESFIDE), that may improve our measurement accuracy by measuring both the R2 and R2* in tissue exhibiting very rapid signal decay [30].

Our study has several limitations. The cohort consisted only of patients with known iron overload and few patients ($n=2$) had liver iron contents in the normal range. Therefore, it is difficult to draw conclusions regarding the association between small and whole liver ROI R2* values

Table 4 Inter-reviewer agreement of liver R2* measurements using a small ROI and whole liver ROI as assessed by the intra-class correlation coefficient (ICC)

Reviewer	Reviewer 2	Reviewer 3
ICC for small ROI		
1	0.99	0.99
2		0.98
ICC for whole liver ROI		
1	0.98	0.99
2		0.98

when the liver iron content is normal. Because the distribution of liver iron is expected to be homogeneous in these children, and because there would be negligible pixel drop-out, there is likely little difference between the two techniques. Also, our study was limited to children with transfusional iron overload and did not include children with hereditary hemochromatosis, cirrhosis or other causes of increased hepatic iron deposition. These other causes of liver siderosis are known to exhibit varying patterns of iron deposition into Kupffer cells, sinusoidal and portal macrophages, epithelial cells and hepatocytes that are disease specific [37, 38]. Therefore, our findings may not be extrapolated to other liver diseases that might demonstrate unique patterns of liver iron distribution and MRI T2 and T2* signal. Also, we evaluated the liver only at the level of the main portal vein and not the areas above or below it, which may have had less pixel drop-out. We chose this approach to provide the MR technologists and reviewers an easily identifiable landmark that was reproducible in all patients.

Conclusion

We found a strong direct association between liver iron content and R2* measurements by small and whole liver ROI methods. Increases in liver R2* values are significantly associated with decreases in fitted pixels within ROIs. In children with transfusional iron overload, pixel drop-out results in an uneven distribution of fitted pixels throughout the liver. This finding becomes obvious on whole liver ROI pixel overlays. In such cases, small ROI R2* measurements can differ substantially, depending on the size, shape and placement of the ROI within the liver. We also found that the range of R2* values and standard errors were smaller using a whole liver ROI technique compared to the small ROI method. In the future, we will use the whole liver ROI technique, whenever possible, to assess our patients with iron overload. A prediction model based on the correlation between liver iron content and R2* values will allow us to estimate patients' liver iron content using R2* measurements. Liver biopsy will be performed only on children who cannot tolerate MRI or have internal metal precluding R2* measurement. In addition, liver

Table 5 Correlation between small and whole liver ROI R2* measurements for each of three reviewers

Reviewer	Correlation coefficient	Standard error	P-value
1	0.99	0.006	<0.0001
2	0.97	0.016	<0.0001
3	0.97	0.018	<0.0001

biopsy will still be necessary when massive hepatic iron deposition precludes accurate R2* measurement using current MRI pulse sequences.

Acknowledgement The authors thank Drs. Fred Hoffer and Robert Gold for performing liver biopsies for this study.

This study was supported in part by NHLBI 5 U54HL070590, Comprehensive Sickle Cell Center, NHLBI 2 U54HL070590-06, Basic Translational Research Program and the American, Lebanese and Syrian Associated Charities

References

- Kushner JP, Porter JP, Olivieri NF (2001) Secondary iron overload. *Hematology Am Soc Hematol Educ Program* 1:47–61
- Chirmomas DS, Geukes-Foppen M, Barry K et al (2008) Practical implications of liver and heart iron load assessment by T2*-MRI in children and adults with transfusion-dependent anemias. *Am J Hematol* 83:781–783
- Hankins JS, McCarville MB, Loeffler RB et al (2009) R2* magnetic resonance imaging of the liver in patients with iron overload. *Blood* 113:4853–4855
- Papakonstantinou O, Alexopoulou E, Economopoulos N et al (2009) Assessment of iron distribution between liver, spleen, pancreas, bone marrow, and myocardium by means of R2 relaxometry with MRI in patients with beta-thalassemia major. *J Magn Reson Imaging* 29:853–859
- Gotsis ED (2008) The uses and differences of R2 and R2* in the determination of iron overload in iron loaded thalassemia patients. *Hemoglobin* 32:75–83
- Wood JC (2007) Magnetic resonance imaging measurement of iron overload. *Curr Opin Hematol* 14:183–190
- Wood JC (2007) Diagnosis and management of transfusion iron overload: the role of imaging. *Am J Hematol* 82:1132–1135
- St Pierre TG, Clark PR, Chua-anusorn W et al (2005) Noninvasive measurement and imaging of liver iron concentrations using proton magnetic resonance. *Blood* 105:855–861
- Wood JC, Enriquez C, Ghugre N et al (2005) MRI R2 and R2* mapping accurately estimates hepatic iron concentration in transfusion-dependent thalassemia and sickle cell disease patients. *Blood* 106:1460–1465
- Gandon Y, Olivie D, Guyader D et al (2004) Non-invasive assessment of hepatic iron stores by MRI. *Lancet* 363:357–362
- Clark PR, Chua-anusorn W, St Pierre TG (2003) Proton transverse relaxation rate (R2) images of liver tissue; mapping local tissue iron concentrations with MRI. *Magn Reson Med* 49:572–575
- Alustiza JM, Artetxe J, Castiella A et al (2004) MR quantification of hepatic iron concentration. *Radiology* 230:479–484
- Anderson LJ, Holden S, Davis B et al (2001) Cardiovascular T2-star (T2*) magnetic resonance for the early diagnosis of myocardial iron overload. *Eur Heart J* 22:2171–2179
- Ernst O, Sergent G, Bonvarlet P et al (1997) Hepatic iron overload: diagnosis and quantification with MR imaging. *AJR* 168:1205–1208
- Papakonstantinou OG, Maris TG, Kostaridou V et al (1995) Assessment of liver iron overload by T2-quantitative magnetic resonance imaging: correlation of T2-QMRI measurements with serum ferritin concentration and histologic grading of siderosis. *Magn Reson Imaging* 13:967–977
- Gandon Y, Guyader D, Heautot JF et al (1994) Hemochromatosis: diagnosis and quantification of liver iron with gradient-echo MR imaging. *Radiology* 193:533–538
- Kaltwasser JP, Gottschalk R, Schalk KP et al (1990) Non-invasive quantitation of liver iron-overload by magnetic resonance imaging. *Br J Haematol* 74:360–363
- Christoforidis A, Perifanis V, Spanos G et al (2009) MRI assessment of liver iron content in thalassamic patients with three different protocols: comparisons and correlations. *Eur J Haematol* 82:388–392
- Olthof AW, Sijens PE, Kreeftenberg HG et al (2008) Non-invasive liver iron concentration measurement by MRI: comparison of two validated protocols. *Eur J Radiol* 71:116–121
- Schwenzer NF, Machann J, Haap MM et al (2008) T2* relaxometry in liver, pancreas, and spleen in a healthy cohort of one hundred twenty-nine subjects-correlation with age, gender, and serum ferritin. *Invest Radiol* 43:854–860
- Virtanen JM, Komu ME, Parkkola RK (2008) Quantitative liver iron measurement by magnetic resonance imaging: in vitro and in vivo assessment of the liver to muscle signal intensity and the R2* methods. *Magn Reson Imaging* 26:1175–1182
- Mavrogeni S, Gotsis E, Ladis V et al (2008) Magnetic resonance evaluation of liver and myocardial iron deposition in thalassemia intermedia and b-thalassemia major. *Int J Cardiovasc Imaging* 24:849–854
- Lam WW, Au WY, Chu WC et al (2008) One-stop measurement of iron deposition in the anterior pituitary, liver, and heart in thalassemia patients. *J Magn Reson Imaging* 28:29–33
- Ooi GC, Chen FE, Chan KN et al (1999) Qualitative and quantitative magnetic resonance imaging in haemoglobin H disease: screening for iron overload. *Clin Radiol* 54:98–102
- Emond MJ, Bronner MP, Carlson TH et al (1999) Quantitative study of the variability of hepatic iron concentrations. *Clin Chem* 45:340–346
- Ambu R, Crisponi G, Scioto R et al (1995) Uneven hepatic iron and phosphorus distribution in beta-thalassemia. *J Hepatol* 23:544–549
- van Deursen C, de Metz M, Koudstaal J et al (1988) Accumulation of iron and iron compounds in liver tissue. A comparative study of the histological and chemical estimation of liver iron. *J Clin Chem Clin Biochem* 26:617–622
- Kreeftenberg HG, Koopman BJ, Huizenga JR et al (1984) Measurement of iron in liver biopsies—a comparison of three analytical methods. *Clin Chim Acta* 144:255–262
- Positano V, Salani B, Pepe A et al (2009) Improved T2* assessment in liver iron overload by magnetic resonance imaging. *Magn Reson Imaging* 27:188–197
- Song R, Cohen AR, Song HK (2007) Improved transverse relaxation rate measurement techniques for the assessment of hepatic and myocardial iron content. *J Magn Reson Imaging* 26:208–214
- Niederer C, Fischer R, Purschel A et al (1996) Long-term survival in patients with hereditary hemochromatosis. *Gastroenterology* 110:1107–1119
- Olivieri NF (2001) Progression of iron overload in sickle cell disease. *Semin Hematol* 38:57–62
- Olivieri NF, Nathan DG, MacMillan JH et al (1994) Survival in medically treated patients with homozygous beta-thalassemia. *N Engl J Med* 331:574–578
- Jorge J (1978) The Levenberg-Marquardt algorithm: implementation and theory. Springer, Berlin, pp 105–116, Lecture notes in mathematics
- Hoffer FA (2000) Liver biopsy methods for pediatric oncology patients. *Pediatr Radiol* 30:481–488
- Stuhne-Sekalec L, Xu SX, Parkes JG et al (1992) Speciation of tissue and cellular iron with on-line detection by inductively coupled plasma-mass spectrometry. *Anal Biochem* 205:278–284
- Batts KP (2007) Iron overload syndromes and the liver. *Mod Pathol* 20(Suppl 1):S31–S39
- Deugnier Y, Turlin B (2007) Pathology of hepatic iron overload. *World J Gastroenterol* 13:4755–4760